Performance Evaluation of the Tolokatsin 2020 Solar Cooker

Eduardo A. Rincón Mejía[1], Eduardo González-Mora[2]

[1] Programa de Energía, Universidad Autónoma de la Ciudad de México, Ciudad de México (México)

[2] Ingeniería en Sistemas Energéticos Sustentables, Facultad de Ingeniería, Universidad Autónoma del Estado de México, Toluca (México)

Abstract

This paper presents the optical performance evaluation of the Tolokatsin-2020, a high-efficiency solar cooker based on nonimaging optics. The design integrates flat and circular absorber Compound Parabolic Concentrator (CPC) profiles, optimized using Bejan's Constructal Law to minimize optical losses by reducing the average number of reflections. A detailed Monte Carlo ray-tracing analysis was performed using SolTRACE software under various conditions, including ideal scenarios and those incorporating realistic optical errors and different solar distributions. The results demonstrate a high and robust optical efficiency of approximately 81% across all tested cases, with minimal performance degradation. The analysis further reveals a homogeneous flux distribution on the receiver and characterizes the system's angular dependence through the Incidence Angle Modifier (IAM). The Tolokatsin-2020 achieves a concentration ratio of 5.8, confirming its potential as a versatile and reliable solution not only for solar cooking but also for other medium-temperature thermal applications such as sterilization, drying, and thermoelectric generation.

Keywords: Solar Cooking, Nonimaging Optics, Constructal Law, Optical Efficiency

1. Introduction

The global community faces the urgent dual challenge of combating famine, which affects an estimated 690 million people, and drastically reducing the reliance on fossil fuels for cooking (United Nations, 2020). Cooking is a universal human necessity that requires a heat source exceeding 100°C (Lecuona et al., 2017). Presently, approximately 28 million people in Mexico depend on burning solid fuels like firewood or charcoal for this purpose—a practice that, on a global scale, affects nearly three billion people (IEA. International Energy Agency, 2018; Rincón Mejía, 2010). The combustion of any fuel for cooking introduces significant hazards, including burns, explosions, poisonings, and widespread environmental contamination. Most critically, household air pollution from these practices results in approximately 3.8 million premature deaths annually (World Health Organization, 2018).

For years, the implementation of solar cookers and ovens has directly addressed these problems by substantially reducing fuel consumption. This technology improves quality of life across all demographics by enabling people to cook food without depending on costly fuels. For populations in poverty, this alleviates the difficult dilemma of prioritizing essential needs.

Current solar cooking technology offers numerous alternatives, as documented by Solar Cookers International (SCI, 2019a). These range from simple devices like the box solar cooker to medium-concentration systems such as parabolic troughs and dishes, and even large Fresnel lenses capable of achieving higher cooking temperatures (Lecuona et al., 2017; SCI, 2019b). While effective, these systems present certain limitations that ongoing research seeks to overcome. Efforts include developing systems with low concentration ratios, such as solar panel cookers and the "funnel" design with its subsequent modifications by Ruivio (Apaolaza-Pagoaga et al., 2021; Solar Cookers International, n.d.), as well as systems with higher concentration ratios, as investigated by Coccia et al. (Coccia et al., 2017). Figure 1 illustrates several examples of these systems.

10.18086/swc.2025.02.22 Available at http://proceedings.ises.org

(a) Solar box **(b) Funnel** **(c) Parabolic dish** **(d) Parabolic trough** **(e) Fresnel lens**

Fig. 1: Main types of solar cookers (Solar Cookers International, 2019)**.**

Recent predictions indicate that reducing the number of reflections in Tolokatsin designs enhances optical efficiency (González-Mora et al., 2020a). To verify this claim, we performed an optical ray-tracing analysis using specialized software to validate the new Tolokatsin-2020 design. Throughout their evolution, Tolokatsin designs have consistently aimed to minimize optical losses while preserving high efficiency and manufacturability. Additionally, we have evaluated the Tolokatsin-2020 design for diverse applications, such as solar-absorption cooling, thermoelectric generation, and drying processes. Section 2 offers a concise overview of the Tolokatsin designs, and Section 3 details the optical analysis methodology, including a brief discussion of the results. This optical analysis provides a foundation for future thermal studies to quantify the figures of merit F_1 and F_2 (Collares-Pereira et al., 2018; Funk, 2000; Funk and Larson, 1998) for this solar cooker.

2. Methodology

2.1. Description of the Tolokatsin 2020

Tolokatsin solar ovens utilize nonimaging optics to achieve efficient radiation transfer from the sun to the receiver, as supported by Winston et al. (2020, 2005). This method prioritizes high optical efficiency while forgoing the formation of a precise solar image, thereby accepting inherent optical aberrations. The geometries of all Tolokatsin designs primarily integrate flat (Eq. 1) and circular absorber (Eq. 2) compound parabolic concentrator (CPC) profiles. This design incorporates the optimum truncation criterion of three times the acceptance angle, initially established by Rincón Mejía et al. (2009), and later demonstrated through Bejan's constructal law (González-Mora and Rincón-Mejía, 2023).

$$\begin{cases} x(t) = \frac{(1+\sin\theta_0)\cos t}{1-\sin(t-\theta_0)} \\ y(t) = \frac{(1+\sin\theta_0)\sin t}{1-\sin(t-\theta_0)} \end{cases}, \quad t \in \left(0, \frac{\pi}{2} - 3\theta_0\right) \qquad \text{(eq. 1)}$$

$$\begin{cases} \begin{cases} x(t) = \sin t - t\cos t \\ y(t) = -(\cos t + t\sin t) \end{cases}, & t \in \left(0, \frac{\pi}{2} + \theta_0\right) \\ \begin{cases} x(t) = \frac{\sin\theta_0\cos(t-\theta_0) - \left(\frac{\pi}{2}+t+\theta_0\right)\cos t}{1+\sin(t-\theta_0)} + \cos\theta_0 \\ y(t) = \frac{\sin\theta_0\cos(t-\theta_0) + \left(\frac{\pi}{2}+t+\theta_0\right)\sin t}{1+\sin(t-\theta_0)} - \sin\theta_0 \end{cases}, & t \in \left(\frac{\pi}{2} + \theta_0, \frac{3\pi}{2} - 3\theta_0\right) \end{cases} \qquad \text{(eq. 2)}$$

Recent work by González-Mora et al. (2020b) demonstrated that applying Bejan's constructal law (Bejan and Llorente, 2008; Rocha et al., 2012) enables the accurate replication of experimental results. This law asserts that "for a finite-size system to persist in time (to live), it must evolve in such a way that it provides easier access to the imposed (global) currents that flow through it." When applied to the Tolokatsin solar cooker concept, the constructal law yielded three principal outcomes: it increased the optical efficiency of the concentrator by reducing the average number of reflections of rays impinging on the absorber, raised the concentration ratio (thereby elevating the stagnation temperature of the absorber), and improved thermal insulation.

Subsequent design evolution, as detailed by González-Mora (2021), involved progressively increasing the number of mirror pairs from one to three. This modification enhanced sunlight redirection by decreasing the average number of reflections and produced a more homogeneous radiation flux over the absorber, even for combinations of single-curvature compound parabolic concentrators (CPCs), as depicted in Fig. 2. The optimized design achieves a concentration ratio of 5.8. Given a receiver tube area of 16.86 cm^2, the corresponding aperture area is 1.621 m^2.

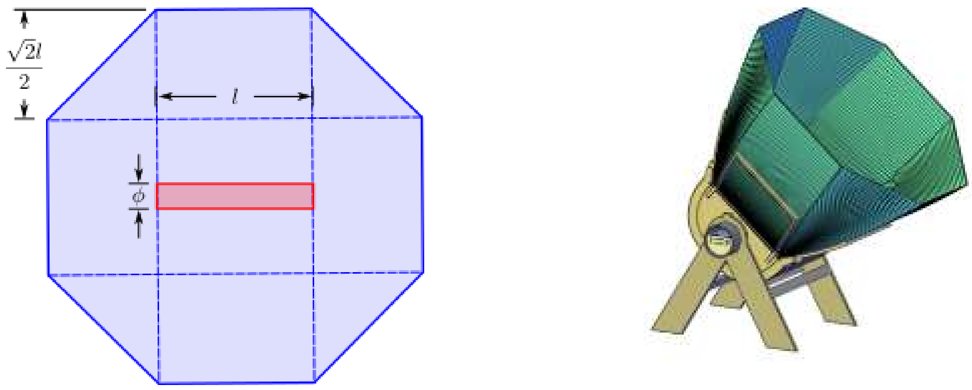

a) Aperture area (b) 3D isometric view

Fig. 2: Tolokatsin-2020 design. Adapted from (González-Mora and Rincón-Mejía, 2021)**.**

2.1. Optical evaluation

It is well known that for CPCs, the power in the receiver depends directly on the average number of reflections N in the optical system by means of a relation $\eta_o \sim \rho^N$. Rabl (1976) have given a description for 2D systems, but for a complex CPC assembly as the Tolokatsin 2020, a raytracing procedure is needed.

Equation 3 defines the optical efficiency, η_o, as the ratio of the heat flux absorbed by the receiver, $\dot{Q}_{rec}$, to the heat flux incident on the aperture of the Tolokatsin-2020 system, $\dot{Q}_{ap}$. The computation of each heat flux depends on the number of rays impinging on the surfaces and the power per ray. This analysis utilized 10 million rays per case, a sample size consistent with that employed by Cooper et al. (2013) and sufficient to achieve an uncertainty of approximately 0.01%.

$$\eta_o = \frac{\dot{Q}'_{rec}}{\dot{Q}'_{ap}} \quad \text{(eq. 3)}$$

In addition, since the 3D system has no symmetry, there is an optical-dependent behavior regarding the incidence angle, thus, the incidence angle modifier (IAM) in the longitudinal and transverse direction are needed (Eq. 4). The IAM, traditionally has been divided into a transverse direction and longitudinal direction, as independent parameters. This can be easily done using SolTrace (Wendelin, 2003).

$$\text{IAM} = \frac{\eta_o(\theta_i)}{\eta_o(\theta_i=0)} = IAM_l \times IAM_t \quad \text{(eq. 4)}$$

2.2. Raytracing procedure

The Tolokatsin-2020 design achieves a concentration ratio of 5.8, incorporating a receiver with a diameter of 16.86 cm and an aperture area of 1.621 m^2. For the optical evaluation of this new design, we implemented a Monte Carlo ray-tracing procedure using SolTRACE software (Wendelin, 2003). This approach employed Zernike polynomials (Doyle et al., 2012), see Eq. 5, to define the optical surfaces, where $B_{i,j}$ represents the polynomial coefficients and N denotes the polynomial degree. The simulation considered the following parameters:

- 0º incidence angle
- The radiation source was modeled as isotopic with 4.65 mrad (pillbox sun shape) and a Gaussian profile with 2.73 mrad
- 0.92 mirror-reflectivity
- 0.94 receiver-absorptivity
- 0.98 glass covers transmissivity
- 3 mrad slope error for the mirrors and 1.95 mrad for the receiver

- 0.5 mrad specularity error
- 1000 W/m^2 DNI

$$z(x,y) = \sum_{i=0}^{N} \sum_{j=0}^{i} B_{i,j} x^j y^{i-j} \quad \text{(eq. 5)}$$

2.3. Estimation of operating and stagnation temperatures

The operating and stagnation temperatures in the absorber can be estimated using a very simple model originally described in a manuscript presented at ASES 2021, held in Boulder, CO. (Rincón Mejía et al., 2021).

Performing a rough energy balance on the absorber of the solar concentrator it is obtained that the useful heat power $\dot{Q}_u$ is approximately:

$$\dot{Q}_u \approx A_c\, G_s\, \eta_o - A_r[\, \varepsilon\, \sigma\, T_r{}^4 + (h\, \Delta T - \kappa\, \nabla T)\,] \quad \text{(eq. 6)}$$

Here:

A_c is the acceptance area,

G_s is an effective solar irradiance on A_c , $G_s \approx (\cos\beta)G_b + \frac{G_d}{C_g}$ (from Rabl, 1976a), where G_b and G_d are the beam and diffuse irradiances, C_g is the geometric concentration and β is the incidence angle

η_o is the optical efficiency

A_r is the absorber exposed area

ε is the emittance of the exterior surface of the absorber

σ is the Stefan-Boltzmann constant

T_r is the effective mean temperature of the exterior surface of the absorber

h is the mean value of the heat transfer coefficient on the external surface of the absorber

κ is the mean value of the thermal conductivity of the insulation

In turn, the optical efficiency is modeled as:

$$\eta_o = f\, \alpha\, \tau\, \rho^{\,N} \quad \text{(eq. 7)}$$

Where:

f is an interception factor, it considers optical errors

α is the absorptance of the exterior surface of the absorber

τ is the transmittance of the transparent cover

ρ is the reflectance of the mirrors

N is the average number of reflections

The average number of reflections N is evaluated following the pionering work of Rabl, (1976); factors f, τ are strongly dependent on the incidence angle of the rays on the acceptation area of the concentrator. The optical analyzes were performed using the US NREL's software SolTrace (González-Mora & Rincón-Mejía, 2021).

These ray-tracing studies have some similarity to those performed by Cooper et al. (2013) on compound parabolic concentrators with polygonal apertures. Besides the energy balances, entropy calculations were made up to optimize the second-law efficiency inspired on early works on this theme.

Thus, the thermal efficiency of the solar concentrator is finally given by:

$$\eta_t = \frac{\dot{Q}_u}{A_c\, G_g} \approx \frac{G_s}{G_g}\, \eta_o - \frac{1}{C_g G_g}\left[\, \varepsilon\, \sigma\, T_r{}^4 + (h\, \Delta T - \kappa\, \nabla T)\,\right] \quad \text{(eq. 8)}$$

where $G_g = G_b + G_d$ is the global irradiance

Introducing the factors j and g, which compare the thermal losses for convection and conduction with that due to the radiation one (thermal radiation is the main and limiting heat loss in solar concentrators), and the ratio of diffuse to global irradiances:

$$j = \frac{(h\,\Delta T - \kappa\,\nabla T)}{\varepsilon\,\sigma\,{T_r}^4} \;\; ; \; g = \frac{G_d}{G_b} \qquad \text{(eq. 9)}$$

$$=> \frac{G_s}{G_g} = \left(\frac{1}{1+g}\right)\left(\frac{(\cos\beta)C_g + g}{C_g}\right) \qquad \text{(eq. 10)}$$

With two limiting cases: a) $g \rightarrow 0$ (there is no diffuse irradiance), => $\frac{G_s}{G_g} \rightarrow \cos\beta$ (eq. 11)

and b) $g \rightarrow \infty$ (there is no beam irradiance), => $\frac{G_s}{G_g} \rightarrow \frac{1}{C_g}$ (eq. 12)

From eq. 8, the mean temperature of the absorber is approximately:

$$T_r \approx \left[\frac{\left(\frac{G_s}{G_g}\eta_o - \eta_t\right) C_g\, G_g}{(1+j)\,\varepsilon\,\sigma}\right]^{\frac{1}{4}} \qquad \text{(eq. 13)}$$

According to eq. 13, thermal efficiency is always lesser than the optical one, which is evidently the governing parameter to be optimised. When $\eta_t \rightarrow 0$, the absorber attains its stagnation temperture T_{stg} which maximum and minimum values, corresponding to the no diffuse irradiance and no beam irradiance, are respectively:

$$T_{stg\,max} \approx \left[\frac{(\cos\beta)\,\eta_o C_g G_g}{(1+j)\,\varepsilon\,\sigma}\right]^{\frac{1}{4}} = \left[\frac{(\cos\beta)\,\eta_o C_g G_b}{(1+j)\,\varepsilon\,\sigma}\right]^{\frac{1}{4}} \text{ and } T_{stg\,min} \approx \left[\frac{\eta_o\,G_d}{(1+j)\,\varepsilon\,\sigma}\right]^{\frac{1}{4}} = \left[\frac{\eta_o\,G_g}{(1+j)\,\varepsilon\,\sigma}\right]^{\frac{1}{4}} \qquad \text{(eq. 14)}$$

3. Results

For the optical simulation, we consider three distinct cases:

- no optical errors,
- inclusion of optical errors with a pillbox solar distribution,
- inclusion of optical errors with a Gaussian distribution.

The optical analysis of the Tolokatsin-2020 solar cooker yielded quantitative performance data across three distinct simulation cases. As summarized in Table 1, the design demonstrates remarkably consistent optical efficiency, approximately 81%, regardless of the inclusion of optical errors or the specific solar irradiance model (pillbox or Gaussian). This consistency underscores the inherent robustness of the nonimaging optical design.

Tab. 1: Results of the optical analysis

Parameter	Case 1 (no errors)	Case 2 (pillbox)	Case 3 (Gaussian)
Average flux, (W/m^2)	3436.32	3434.21	3435.44
Peak flux, (W/m^2)	17839	16392.9	16372.7
Optical efficiency, (%)	81.09	81.03	81.02

The flux maps presented in Fig. 4 provide a visual confirmation of this performance. While the peak flux values understandably decrease when optical errors are introduced—dropping from ~17 W/ m^2 in Case 1 to ~16 W/ m^2 in Cases 2 and 3—the overall spatial distribution of energy on the receiver remains stable. This homogeneous flux distribution is a key attribute for efficient thermal performance and mitigates the risk of localized hot spots that could damage the receiver.

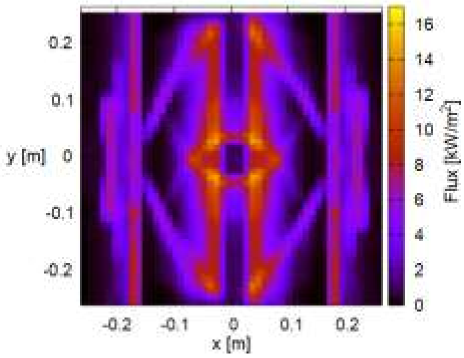

a) Case 1

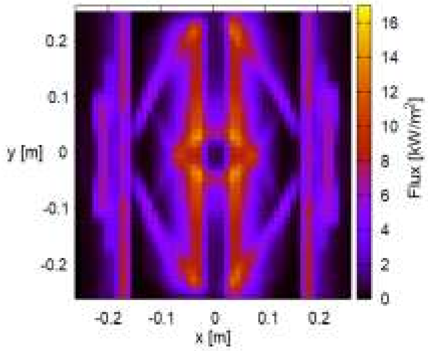

(b) Case 2

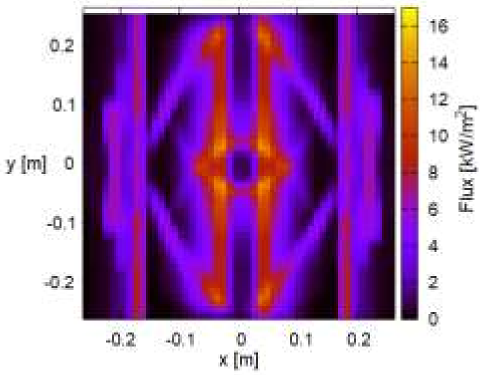

(c) Case 3

Fig. 4: Flux maps on the Tolokatsin-2020 absorber

The performance under off-axis angles is characterized by the IAM, shown in Fig. 5. The optical efficiency remains high for incidence angles below 10°, with a more pronounced decline in the transverse direction. The system's acceptance angle is defined as 15.78°, beyond which the optical efficiency falls to zero, confirming the design's alignment with the theoretical acceptance angle of the CPC profiles. This predictable angular performance is critical for informing user operation and tracking strategies.

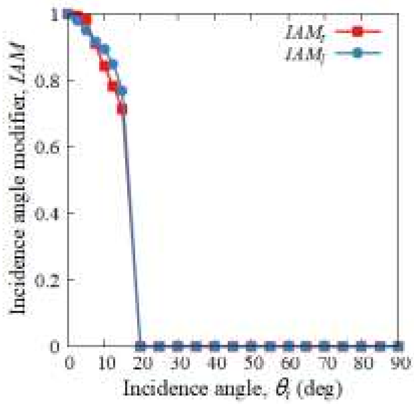

Fig. 5: Incidence angle modifier for the Tolokatsin 2020.

The consistent behavior observed across all cases can be attributed to the fundamental principles of nonimaging optics, specifically the conservation of etendue and Fermat's principle, which govern the deterministic and efficient propagation of light rays through the system (Winston et al., 2020).

4. Conclusions

The optical evaluation of the Tolokatsin-2020 solar cooker confirms the successful implementation of its nonimaging optical design, refined through the application of the Constructal Law. The system demonstrates a high peak optical efficiency of 81.09%, which remains exceptionally stable under simulations that introduce realistic optical errors and different solar irradiance models. This consistency underscores the design's robustness and its insensitivity to common manufacturing and operational imperfections. Furthermore, the ray-tracing analysis reveals a homogeneous radiation flux on the receiver, a critical characteristic for uniform heating and effective thermal energy transfer.

The high performance validates the design evolution guided by Constructal Law, which successfully reduced the average number of reflections to provide easier paths for radiative energy flow. The Tolokatsin-2020, with a concentration ratio of 5.8 and a well-defined acceptance angle, establishes its practical viability as a high-performance solar thermal technology. This work confirms the cooker's potential not only for solar cooking but also for its application in other medium-temperature processes such as sterilization, drying, and thermoelectric generation, providing a solid foundation for future thermal performance characterization.

5. References

Apaolaza-Pagoaga, X., Sagade, A.A., Rodrigues Ruivo, C., Carrillo-Andrés, A., 2021. Performance of solar funnel cookers using intermediate temperature test load under low sun elevation. Solar Energy 225, 978–1000. https://doi.org/10.1016/j.solener.2021.08.006

Bejan, A., Llorente, S., 2008. Design with Constructal Theory. John Wiley & Sons, Inc., Hoboken, NJ, USA. https://doi.org/10.1002/9780470432709

Coccia, G., Di Nicola, G., Pierantozzi, M., Tomassetti, S., Aquilanti, A., 2017. Design, manufacturing, and test of a high concentration ratio solar box cooker with multiple reflectors. Solar Energy 155, 781–792. https://doi.org/10.1016/J.SOLENER.2017.07.020

Collares-Pereira, M., Cavaco, A., Tavares, A., 2018. Figures of merit and their relevance in the context of a standard testing and performance comparison methods for solar box – Cookers. Solar Energy 166, 21–27. https://doi.org/10.1016/j.solener.2018.03.040

Cooper, T., Dähler, F., Ambrosetti, G., Pedretti, A., Steinfeld, A., 2013. Performance of compound parabolic concentrators with polygonal apertures. Solar Energy 95, 308–318. https://doi.org/10.1016/j.solener.2013.06.023

Doyle, Ke., Genberg, V., Michels, G., 2012. Zernike and Other Useful Polynomials, in: Integrated Optomechanical Analysis, Second Edition. Society of Photo-Optical Instrumentation Engineers. https://doi.org/10.1117/3.974624.ch3

Funk, P.A., 2000. Evaluating the international standard procedure for testing solar cookers and reporting performance. Solar Energy 68, 1–7. https://doi.org/10.1016/S0038-092X(99)00059-6

Funk, P.A., Larson, D.L., 1998. Parametric model of solar cooker performance. Solar Energy 62, 63–68. https://doi.org/10.1016/S0038-092X(97)00074-1

González-Mora, E., 2021. Evolution and further improvement opportunities of a non-imaging optics solar cooker design. Academia Letters. https://doi.org/10.20935/AL3184

González-Mora, E., Rincón-Mejía, E.A., 2023. A Simple Truncation Criterion in CPCs Using Constructal Theory, in: 36th International Conference on Efficiency, Cost, Optimization, Simulation and Environmental Impact of Energy Systems (ECOS 2023). ECOS 2023, Las Palmas De Gran Canaria, Spain, pp. 1678–1688. https://doi.org/10.52202/069564-0152

González-Mora, E., Rincón-Mejía, E.A., 2021. Optical Evaluation of the Tolokatsin-2020 High-Efficiency Solar Cooker, in: Proceedings of the ISES Solar World Congress 2021.

González-Mora, E., Rincón-Mejía, E.A., Morillón Gálvez, D., 2020a. Diseño constructal de CPCs y la evolución de los diseños Tolokatsin, in: Gonçalves, H., Romero, M. (Eds.), XVII Congreso Ibérico y XIII

Congreso Iberoamericano de Energía Solar. Lisboa, pp. 131–136. https://doi.org/https://doi.org/10.34637/cies2020.1.2013

González-Mora, E., Rincón-Mejía, E.A., Morillón Gálvez, D., 2020b. Diseño constructal de CPCs y la evolución de los diseños Tolokatsin, in: XVII Congreso Ibérico y XIII Congreso Iberoamericano de Energía Solar. Lisboa, pp. 131–136. https://doi.org/https://doi.org/10.34637/cies2020.1.2013

IEA. International Energy Agency, 2018. World Energy Outlook 2018 [WWW Document]. URL https://www.iea.org (accessed 2.24.19).

Lecuona, A., I. Nogueira, J., Rodríguez Aumente, P., Legrand, M., 2017. Solar Cooking for All, in: Rincón-Mejía, E., De las Heras, A. (Eds.), Sustainable Energy Technologies. CRC Press, pp. 255–276.

Rabl, A., 1976. Optical and thermal properties of compound parabolic concentrators. Solar Energy 18, 497–511. https://doi.org/10.1016/0038-092X(76)90069-4

Rincón Mejía, E.A., 2010. Aplicaciones de la óptica anidólica en concentradores solares.

Rincón Mejía, E.A., Durán García, M.D., Lentz Herrera, Á., 2009. New Solar Air Heater Based on Non-Imaging Optics for High-Temperature Applications, in: ASME 2009 3rd International Conference on Energy Sustainability, Volume 2. pp. 839–844. https://doi.org/10.1115/ES2009-90306

Rincón Mejía, E.A., Rincón Rubio, A.G., Rincón Rubio, V.A., 2021. Nonimaging Optics and Constructal Law Towards Optical Solar Cookers, in: ASES SOLAR2021 Proceedings, USA, doi:10.18086/solar.2021.01.03. htpp://proceedings.ises.org

Rocha, L.A.O., Llorente, S., Bejan, A., 2012. Constructal Law and the Unifying Principle of Design, Understanding Complex Systems. Springer New York.

SCI, 2019a. Solar Cookers International [WWW Document]. URL https://www.solarcookers.org/ (accessed 2.24.19).

SCI, 2019b. Solar Cookers International [WWW Document]. URL https://www.solarcookers.org/ (accessed 2.23.19).

Solar Cookers International, 2019. Solar cooker designs [WWW Document]. URL https://solarcooking.fandom.com/wiki/Category:Solar_cooker_designs (accessed 8.14.21).

Solar Cookers International, n.d. Fun-Panel [WWW Document]. URL https://solarcooking.fandom.com/wiki/Fun-Panel (accessed 8.13.21).

Wendelin, T., 2003. SolTRACE: A New Optical Modeling Tool for Concentrating Solar Optics, in: Solar Energy. ASMEDC, pp. 253–260. https://doi.org/10.1115/ISEC2003-44090

Winston, R., Jiang, L., Oliker, V., 2020. Nonimaging Optics: Solar and Illumination System Methods, Design, and Performance. Crc Press.

Winston, R., Miñano, J., Benítez, P., 2005. Nonimaging optics, 1st ed. Elsevier, New Jersey.

World Health Organization, 2018. Household air pollution and health Key Facts. Fact Sheets.